SUPPLEMENTARY APPENDIX

SUPPORTING MATERIALS AND METHODS

Animals

C57BL/6J (B6), PWD/PhJ (PWD), and B6.Chr^{PWD} consomic mice were purchased from Jackson Laboratories (Bar Harbor, Maine, USA), then bred and housed in a single room within the vivarium at the Larner College of Medicine at the University of Vermont for 2-4 generations prior to any experimentation. B6.Chr10.1^{PWD} mice were not included in the study due to poor breeding performance. The experimental procedures used in this study were approved by the Animal Care and Use Committee of the University of Vermont.

To ensure their correct identity, and to enhance rigor and reproducibility of these studies, B6.Chr^{PWD} consomic mice were subjected to genome-wide SNP genotyping using DartMouse genotyping services (Dartmouth College, NH USA). All mice used in this study were of the expected genotypes, with the following exceptions. B6.Chr4^{PWD} mice were found to be a mix of various B6/PWD genotypes on Chr4, where various regions of the Chr4^{PWD} had been replaced with B6 genome. Chr17^{PWD} mice were found to carry a homozygous B6-derived interval between 30 – 45 Mb on Chr17, encompassing *H2*, as we have previously reported (1).

Induction and evaluation of EAE

EAE was induced in B6 and B6.Chr^{PWD} consomic mice using the 2×MOG$_{35-55}$/CFA protocol, as previously described (2). Mice were injected subcutaneously with 0.1 ml of emulsion containing 0.1 mg of myelin oligodendrocyte glycoprotein peptide 35-55 (MOG$_{35-55}$) peptide (Anaspec Inc., MA, USA) in PBS and 50% complete Freund's adjuvant (CFA; Sigma, USA) on day 0 on the lower flanks (50 µl per flank), followed by an identical injection on upper flanks on day 7. CFA was supplemented with an additional 4 mg/ml *Mycobacterium tuberculosis* H37Ra (Difco, USA). As an alternative method for EAE induction, B6 and PWD mice were immunized with 2.5 mg of mouse spinal cord homogenate emulsified in CFA on D0 and D7, followed by i.p. administration of 200 ng pertussis toxin (PTX) on D0 and D2. Starting on day 10, mice were scored visually, as follows: 1 – loss of tail tone, 2 - loss of tail tone and weakened hind limbs, 3 - hind limb paralysis, 4 - hind limb paralysis and incontinence, 5 - quadriplegia or death. EAE scoring was performed by a non-biased or blinded observer whenever possible. Cumulative disease score (CDS) was calculated as the sum of all daily scores over the course of 30 days (3, 4) and significance of differences was determined by Kruskal-Wallis with Dunn's post-hoc comparisons. Significance of differences in disease course were determined using Friedman's non-

parametric two-way ANOVA, as previously described (2), using the treatment*time interaction term to evaluate differences. Since the different experiments described in the manuscript were carried out over a time period encompassing ~5 years, some variability in EAE severity (likely owing to different reagents, preparations, and environmental variables) is apparent across different experiments, and is expected. Specifically, the apparently low EAE in B6+B6 co-housed controls in **Fig. 7B** may be due to variation in these aforementioned factors and/or the result of the stress introduced by co-housing. However, all experimental comparisons were only performed between groups that were studied in parallel to mitigate confounding effects of EAE induction variability.

Microbial DNA isolation and 16S DNA sequencing

Fecal samples were collected by placing individual mice into empty cages without bedding and waiting for them to defecate. 1-2 fecal pellets were collected per mouse, briefly stored on ice, followed by long-term storage at -80°C until extraction. Cecal samples were collected as described below (see Microbial transplantation), and stored at -80°C until extraction. DNA was extracted from the fecal pellets or cecal contents using the MoBio PowerSoil extraction kit (MoBio, USA). DNA quality and quantity was assessed by NanoDrop and Qubit instruments, as well as by agarose gel electrophoresis.

16S rRNA gene amplicon generation and sequencing was performed at the University of Illinois W.M. Keck Center for Comparative and Functional Genomics, as follows. 16S amplicon libraries were generated using the Fluidigm Access Array (Fluidigm,USA) amplification according to standard manufacturer's protocols. The following primer sequences were used to generate V3-V4 amplicons, with the underlined region representing the unique targeted regions, and the remainder of the sequence representing Fluidigm-specific adapters (V3-357F, ACACTGACGACATGGTTCTACA<u>CCTACGGGNGGCWGCAG</u> V4-805R, TACGGTAGCAGAGACTTGGTCT<u>GACTACHVGGGTATCTAATCC</u>). The final 14 Fluidigm pools were transferred from the Functional Genomics laboratory to the DNA Services laboratory of the Roy J. Carver Biotechnology Center at the University of Illinois at Urbana-Champaign. The final pools were quantitated using Qubit (Life Technologies, Grand Island, NY) and then further quantitated by qPCR on a BioRad CFX Connect Real-Time System (Bio-Rad Laboratories, Inc. CA). The pool was mixed evenly based on the qPCR values, then size selected on 2% eGel (Invitrogen) for the products 400-800nt and 200-400nt in size. qPCR was repeated on the two sized pools and the final pool was made by mixing the under 400nt products with the over 400nt products in a ratio of 1:20, respectively, according to the qPCR value. This final pool was then denatured and spiked with

20% indexed PhiX control library and loaded onto HiSeq V2 or MiSeq flowcells at a concentration of 10 pM for cluster formation and sequencing. The libraries were sequenced from both ends of the molecules to a total read length of 250nt from each end. The run generated .bcl files which were converted into demultiplexed compressed fastq files using bcl2fastq 2.17.1.14 (Illumina, CA). A secondary pipeline decompressed the fastq files, generated plots with quality scores using FastX Tool Kit, and generated a report with the number of reads per sample/library. The .bcl files were also processed in bcl2fastq 2.17.1.14 without demultiplexing, then sorted by initial PCR-specific primer using a custom in-house pipeline. The entire set of sequencing data was submitted to the NCBI Sequence Read Archive under the BioProject ID PRJNA590851.

16S data preprocessing, OTU assignment, and diversity analyses

Raw sequencing reads (fastq format) were merged using *fastq_mergepairs* as implemented in VSEARCH (version 2.5.0; fastq_maxdiffs set to 2, fastq_minovlen = 30) (5). Resulting contigs were filtered for low quality reads (VSEARCH: *fastq_filter*; fastq_maxee = 0.5) and chimeric sequences were identified and removed using the UCHIME algorithm (VSEARCH: *uchime_ref*; reference database rdp gold v9) (6). Operational taxonomic units (OTUs) were identified using the *UPARSE* algorithm (default parameters) as implemented in USEARCH version 10.0.240 and taxonomic classification was performed on resulting OTUs applying the SINTAX algorithm (USEARCH; reference database RDP 16s training set V16) (7-9). The OTU table was created using *usearch_global* (VSEARCH; 97% identity). To create a phylogenetic tree, OTUs were aligned using MOTHUR version 1.39.5 (*align.seqs* command; SILVA v123 as reference database) and tree reconstruction was performed using FASTTREE version 2.1.4 with a generalized time-reversible (GTR) substitution model, and the gamma option to rescale branch length (10, 11). The final tree was rooted using midpoint rooting.

The preprocessed 16S data was rarefied to correct for differences in read depth between samples. The consomic dataset was rarefied to 7,000 reads, the GMT experiment data to 10,000, and the cohousing experiment data to 12,000 reads, respectively.

Alpha diversity (Shannon-diversity, Chao1) was estimated using the R *vegan* package (version 2.5-3). Additionally, Faith's phylogenetic distance was estimated using the *picante* package version 1.7 (12). Beta diversity was estimated using Bray-Curtis dissimilarity (*vegdist* as implemented in *vegan*) and (weighted/unweighted) UniFrac distance (*phyloseq* package version 1.26.1) (13). Multivariate analysis of

variance using distance matrices were performed using the Adonis test (*vegan*; 9,999 permutations). Multivariate homogeneity of group dispersions was assessed using *betadisper* (*vegan*) on UniFrac distance using the spatial median with adjustment for small sample bias and adding a constant to avoid non-negative eigenvalues.

Indicator species were identified using statistical significance of species site-group associations as implemented in the *indicspecies* R package (v1.7.6) with 9,999 permutations, with a cutoff of $P_{corr}<0.1$ (P-values were corrected using Šidák correction). Random forest regression was performed using the R package *caret* (v6.0-84) using 10-fold cross-validation repeated 10 times (using 80% of the data as training set). To reduce the computational burden, only OTUs with at least 0.01% of the total abundance were selected. For each variable (OTU) present in the model, its relative importance for classification was estimated using the *varImp* function as implemented by the *caret* package.

All statistical analyses were performed using R version 3.5.1. Correlations were estimated using rank-based statistic (Spearman correlation) and resulting P-values were corrected using Benjamini-Hochberg correction. Significance was assessed using Mann-Whitney *U* test or Kruskal-Wallis test with post-hoc testing (Dunn-test with Benjamini-Hochberg correction for multiple testing) depending on the data distribution and number of groups. Differential microbial abundance analysis was performed using *DESeq2* (14) (default parameters) as implemented in the MicrobiomeAnalyst software (15), with a cut-off filter of an log2(fold change) ≥ |1| and $P_{corr} < 0.05$.

Analyses of EAE CDS association with microbial abundance and function

Microbiome Regression-based Kernel Association Test (MiRKAT) was used to test for associations between EAE CDS phenotypes and associated microbiome structure (OTU abundance) across all of the B6.Chr^{PWD} consomic strains, as follows (16). For each consomic strain, we calculated an average EAE CDS for each strain, as well as average OTU abundance for each OTU. Next, Spearman correlations were calculated for all OTUs with CDS and significant correlations were selected for further analysis ($P_{adj} < 0.01$). For significant correlated OTUs, MiRKAT was applied as implemented in the R package *MiRKAT* version 1.0.1 with Bray-Curtis dissimilarity kernel to estimate a P-value (9,999 permutations), using sex and strain as co-variates.

Functional profiles of 16S data were inferred using PICRUSt2 (version 2.1.4-b; maximum NSTI set to 0.3, minimum number of reads across all samples set to 20, minimum number of samples per OTU set to 5) and

KEGG IDs were matched to gene names (*R::KEGGREST* version 1.22.0) (17). Enrichment of GO terms (Molecular Function and Biological Process, database versions 2018) associated with the KEGG ID matched genes was assessed using the R package *enrichR* (version 2.1) for positively and negatively associated (Spearman correlation; $P < 0.05$) KEGG IDs (18). Combined enrichment scores ($c = log(p) * z$ where p refers to P-value from Fisher exact test and z is the z-score computed by assessing the deviation from the expected rank) and P-values for enrichment were calculated.

Gene set variation analysis (GSVA) was performed using the R package *GSVA* (version 1.32.0) on a customized gene set list and a minimum size of 7 (19). The customized gene set list was created using PICRUSt2 functional predictions on OTUs associated with CDS (described above; total 203 OTUs). First, KEGG pathways were extracted for each KEGG ID. Next, orthology terms (gene names) were retrieved for each KEGG pathway (using *KEGGREST*). Finally, GSVA was performed using abundance estimates from PICRUSt2 and results were visualized using the R package *ComplexHeatmaps* version 2.0.0 and row-scaling (20).

Microbiome transplantation and cohousing

The gut microbiome transplantation (GMT) protocol was based on a procedure developed by Blaser and colleagues (21). Donor mice were euthanized by CO_2 inhalation. To minimize the exposure of gut contents to oxygen, the cecum was tied off at the proximal and distal ends, removed and stored on ice briefly, and transferred to an anaerobic chamber (Coy Labs, Inc, USA). The cecum was dissected open and contents were flushed out with and resuspended in liquid dental transport medium (Anaerobe Systems, CA, USA), with pre-reduced dilution blank saline (Anaerobe Systems, CA, USA) added to adjust the final volume. A small portion of the cecal contents was pelleted and frozen for DNA extraction and 16S analysis. 100% sterile glycerol was added to the remainder of the sample to a final concentration of 20%. The samples were aliquoted into Hungate tubes (Fisher Scientific, USA), flash frozen in a dry ice/ethanol bath, and stored at -80°C until use. Cecal contents from 3-4 donor mice were pooled by sex/strain, in 4 ml final volume per cecum.

For inoculation, GMT recipient germ-free (GF) 4-5 week old C57BL/6J mice were purchased from the National Gnotobiotic Rodent Resource Center at University of North Carolina School of Medicine (Chapel Hill, NC, USA). Mice were shipped in sterile crates, and crates were opened in a laminar flow hood followed by immediate inoculation of the recipient mice. Inoculation was performed by gastric gavage with 0.125 ml of

cryopreserved cecal contents. Inoculated mice were maintained under barrier conditions with sterilized food, water and caging, with handling minimized to ensure minimal introduction of additional microbes or cross-contamination. After a 4-week stabilization period, inoculated mice were either used for EAE experiments directly, or served as founder breeding pairs for vertical transmission of the gut microbiome, as described in the Results section.

For colonization with *L. reuteri*, GMT was performed as above, with the following modifications. 4-week old recipient B6-GF mice received 200 µl of B6 cryopreserved cecal content via oral gavage to establish two breeding pairs per microbiome. Separate breeding pairs received 100 µl of B6 cecal content supplemented with 100 µl *L. reuteri* at 10^9 CFU. Fecal samples were collected 4-weeks post-gavage for qPCR and 16S analysis.

Lactobacillus species identification, quantification, and isolation

Species-specific qPCR primers for *L. reuteri* and *L. murinus* were based on those previously described (22-24). For quantification of relative species abundance, total fecal DNA was subjected to SYBR-Green based qPCR using the Dynamo ColorFlash kit (Thermofisher, Inc, USA). A second set of pan-eubacteria specific primers (22) was used to normalize the species-specific signal by total bacterial content.

For *Lactobacillus reuteri* isolation, total cecal contents harvested from a PWD mouse was resuspended in 50 ml MRS medium (Thermofisher, Inc, USA) supplemented with 0.25g/L L-cysteine, 20µg/ml vancomycin and adjusted to pH 5. Contents were incubated anaerobically overnight at 37˚C, 200 rpm to select for vancomycin-resistant species and allow for overgrowth. The resulting cultures were streaked for isolation onto agar medium of the same formulation. Single colonies were selected based on morphology consistent with lactic acid bacteria, cultured overnight in 5 ml MRS medium of the same formulation and cryopreserved, followed by DNA extraction through standard boiling preparation, and screening by qPCR using species-specific primers. Positive clones were recovered from glycerol stocks, cultured in vancomycin-free medium to confirm purity based on morphology and repeat qPCR analysis. For colonization studies, three isolates per species were grown to log-phase, adjusted to OD_{600}=0.5 with fresh culture medium, mixed at equal volumes, and cryopreserved followed by repeat qPCR validation of each pooled stock. Fresh pooled log-phase cultures were cryopreserved for final use in colonization studies with colony forming units (CFU) quantified by serial dilution and plating both prior to storage and post-gavage.

Flow cytometry

For characterization of CNS-infiltrating cells, EAE was induced as described above. At day 30 post-induction, mice were deeply anesthetized by isoflurane inhalation, perfused transcardially with PBS, and spinal cords were removed. Spinal cords were homogenized using a Dounce glass homogenizer, and a single cell suspension was obtained and passed through a 70 μm strainer. Mononuclear cells were obtained by Percoll gradient (37%/70%) centrifugation and collected from the interphase. For intracellular cytokine analysis, cells were washed and stimulated with 5 ng/ml of PMA and 250 ng/ml of ionomycin in the presence of brefeldin A (Golgi Plug reagent**,** BD Bioscience) for 6 hours. Cells were labeled with the UV-Blue Live/Dead fixable stain (Thermofisher, USA) followed by surface staining with antibodies against CD45, CD11b, CD4, CD8, TCRγδ, and TCRβ (Biolegend, USA). Afterwards, cells were fixed, permeabilized with 0.2% saponin, and labeled with anti-IL-17A, anti-IFNγ, and anti-GM-CSF antibodies (Biolegend, USA). All antibodies were directly conjugated to fluorophores. Labeled cells were analyzed using an LSRII flow cytometer (BD Biosciences). Compensation was calculated using appropriate single color controls. Data were analyzed using FlowJo software, version 10 (Tree Star Inc, Ashland, OR).

For characterization of peripheral MOG-specific T cell responses, mice were immunized using the 2×MOG_{35-55}/CFA protocol as above, and spleens were harvested at day 10 post-immunization. Total splenocytes were resuspended in RPMI 1640 supplemented with 5% fetal bovine serum and stimulated with 50 μg/ml of $MOG_{35–55}$ for 3 days, followed by a 4 hour restimulation with PMA and Ionomycin in the presence of Golgi Plug, followed by flow cytometry and intracellular cytokine staining, as above.

For characterization of naive T cell responses, spleens were collected from 8-10 week old mice and stimulated directly ex vivo with PMA and Ionomycin in the presence of Golgi Plug, followed by flow cytometry and intracellular cytokine staining, as above.

Metabolomics

Serum samples were collected from GMT recipients at day 30 post-EAE induction, stored at -80°C, and shipped on dry ice to the mass spectrometry facility at University of Colorado, Denver. Metabolomic analysis was performed essentially as described previously (25). Briefly, serum samples were thawed on ice and then 20

uL of serum was diluted with 480 uL of ice-cold methanol:acetonitrile:water (5:3:2, v/v/v). Samples were vortexed 30 min at 4°C, then clarified by centrifugation and supernatants analyzed on a Thermo Vanquish UHPLC coupled online to a Thermo Q Exactive mass spectrometer using a 5 min C18 gradient method as described (25). Metabolite assignments and peak area measurements were performed using Maven (Princeton University) against an in-house standard library. Instrument stability and quality control was assessed as described (26, 27) using technical replicate injections every 6 runs.

Data were analyzed using MetaboAnalyst, version 4.0 (28). Outliers were identified using the built-in random forest outlier identification function combined with heatmap and PCA visual inspection of data, which resulted in the exclusion of 2 samples, one from each experimental group. Data and analysis without outlier exclusion are presented in **Dataset S4 E-H**. Differentially abundant metabolites were identified using a threshold of $P \leq 0.05$, with heatmap clustering based on Euclidean distance and Ward's linkage. Built-in KEGG pathway analysis with the human pathway library was implemented in MetaboAnalyst using the top 23 differentially abundant metabolites as an input list, a hypergeometric test for over-representation analysis, and relative betweenness centrality as the importance measure for topological analysis.

SUPPLEMENTAL FIGURE LEGENDS

Figure S1. Gut microbial taxonomic distribution of wild-derived PWD, inbred B6 and B6.Chr^{PWD} consomic mice. Extended data comparing the gut microbial composition and diversity in PWD and B6 mice. Distribution of phyla (**A**), family (**B**) and genera (**C**) comprising the bacterial 16S reads. Each bar represents an individual mouse, parental breeding pairs are annotated along the x-axis with experimental housing cage annotation at the top of each bar with a total of 32 B6 (17 female and 15 male) and 19 PWD (10 female and 9 male) mice, with all 16S data rarefied to 7,000 reads. Comparison of microbiomes across the B6.Chr^{PWD} consomic strains (including B6 and PWD parental strains) with distribution of phyla (**D**), family (**E**) and genera (**F**) comprising bacterial 16S reads rarefied to 7,000 reads. Each bar represents the average distribution for each consomic strain and is annotated with the total number individuals per strain along the top.

Figure S2. Additional beta diversity analyses of PWD and B6 fecal and cecal microbiomes. DNA isolated from fecal samples collected from 8-14 week old B6 and PWD mice was subjected to 16S rRNA gene sequencing and analysis, as described in the Methods section. Beta diversity of OTU abundance was measured using (**A**) Bray-Curtis dissimilarity (Strain: R^2=0.39, P<0.001; Strain:Sex R^2=0.03, P=0.20) and (**B**) weighted UniFrac distance (Strain: R^2=0.37, P<0.001; Strain:Sex R^2=0.02, P=0.44). Beta diversity of fecal and cecal DNA samples isolated from the same individual mice as assessed by (**C**) Bray-Curtis dissimilarity and (**D**) weighted UniFrac distance. Samples from individual mice of each strain are designated by corresponding numbers.

Figure S3. Identification of gut microbial species and functions associated with EAE severity in the B6.Chr^{PWD} consomic model. (**A**) A schematic of the analysis pipelines used for the integration of 16S microbial abundance data (obtained as described in **Fig. 2**) and EAE outcomes (obtained as described in **Fig. 3**) in B6.Chr^{PWD} consomic mice. (**B**) Multivariate analysis of associations between EAE CDS and microbial abundance. MiRKAT analysis was performed on 16S OTU abundance data and EAE CDS for B6 mice and each of the 27 B6.ChrPWD consomic strains, as detailed in the Methods section. A heatmap indicating abundance (scaled log(abundance+1)) of the 203 significantly associated OTU across each of the 27 consomic strains and B6, shown in columns (strains are arranged from left to right from low to high CDS, indicated across the top), and significantly associated OTU are shown in in rows. The strength and direction of the association (Spearman's Rho) is indicated on the left side, with positive Rho values indicating increased abundance associating with high EAE CDS, and vice versa.

Figure S4. Diagrams of experimental microbiome manipulation and breeding schemes. (**A**) Ex-germ-free mice receiving either B6 or PWD fecal microbiome transplantation, denoted B6→B6-GF or PWD→B6-GF as in **Fig. 5A** and **B,** served as G_0 breeding pairs for the vertical transmission model (**B**) as in **Fig. 5C**, denoted G_1:B6→B6-GF or G_1:PWD→B6-GF. (**C**) Cohousing-mediated bidirectional microbiota transfer between B6 and PWD mice (related to **Fig. 7**). (**D**) *L. reuteri* transplantation and vertical transmission model (related to **Fig. 8** and **9**).

Figure S5. Divergence between B6 and PWD gut microbial composition is consistent between consomic, fecal microbiome transfer, and cohousing experiments. (**A**) Combined beta diversity analysis by unweighted UniFrac distance of fecal microbiomes of B6 and PWD in consomic (**Fig. 1-2**), GMT (**Fig. 5**) and cohousing (**Fig. 7**) experiments.

Figure S6. Quantification of *Lactobacillus* Transmission by cohousing and GMT models. Relative abundance of *L. reuteri* and *L. murinus* was determined by 16S analysis (**A**) or by species-specific qPCR (**B**) across the different experimental groups in the cohousing model as in **Fig. 7**. Relative abundance of *L. reuteri* and *L. murinus* between B6 and PWD donors and ex-GF B6 and PWD microbiome recipients in the direct GMT model (**C**) or the vertical transmission model (**D**), as determined by species-specific qPCR

Figure S7. Colonization with L. reuteri is sufficient to modulate EAE susceptibility and encephalitogenic T cell responses. Cells were isolated from the CNS as in **Fig. 8**. (**A**) Percentage of TCR-β^+ $CD8^+$ cells positive for the indicated cytokines. Representative flow cytometry plots (for **Fig. 8D** and panel **A**) are shown in **B-D**. The percentages of cells positive for a given single cytokine indicate cells positive for the cytokine independent of coproduction of the other three cytokines (thus including single, double, and triple producers), whereas the double-positive percentages indicate cells producing specifically both of the indicated cytokines.

Figure S8. Colonization with *L. reuteri* enhances $CD4^+$ and $CD8^+$ T cell inflammatory cytokines production in naïve and day 10 immunized mice. Founder G_0 GF B6 mice were inoculated with cecal contents from B6 donors, supplemented or not with 10^9 CFU of *L. reuteri* to establish breeding pairs for vertical transmission. (**A-B**) Total splenocytes were isolated from naïve G_1 offspring at 8-12 weeks, restimulated for 4 hrs PMA and ionomycin in the presence of Golgi Plug, and analyzed by flow cytometry as described in Supplemental Methods. (**C-D**) 8-12 week mice were immunized with $2^x MOG_{35-55}$/CFA, followed by splenocyte isolation on day 10 post-immunization. Splenocytes were cultured in the presence of 50 μg/ml of MOG35-55 for 3 days, followed by restimulation with PMA and ionomycin in the presence of Golgi Plug, and analyzed by flow cytometry, as above. Shown are the percentages of TCRβ^+ $CD4^+$ (**A** and **C**) and TCRβ^+ $CD8^+$ (**B** and **D**) cells positive for the indicated cytokines.

Figure S9. Partial transfer of gut microbiota from B6 to PWD mice by cohousing is sufficient to modulate EAE. 3-week-old PWD mice were randomized to be cohoused with sex- and age-matched B6 mice, or a different litter of age-matched PWD mice as controls. At 5-6 weeks post-cohousing, EAE was induced by immunization with spinal cord homogenate in CFA + PTX (see Supplementary Materials and Methods). Clinical disease course (**A**) and cumulative disease score (**B**) are shown.

SUPPLEMENTAL FIGURES

Figure S1

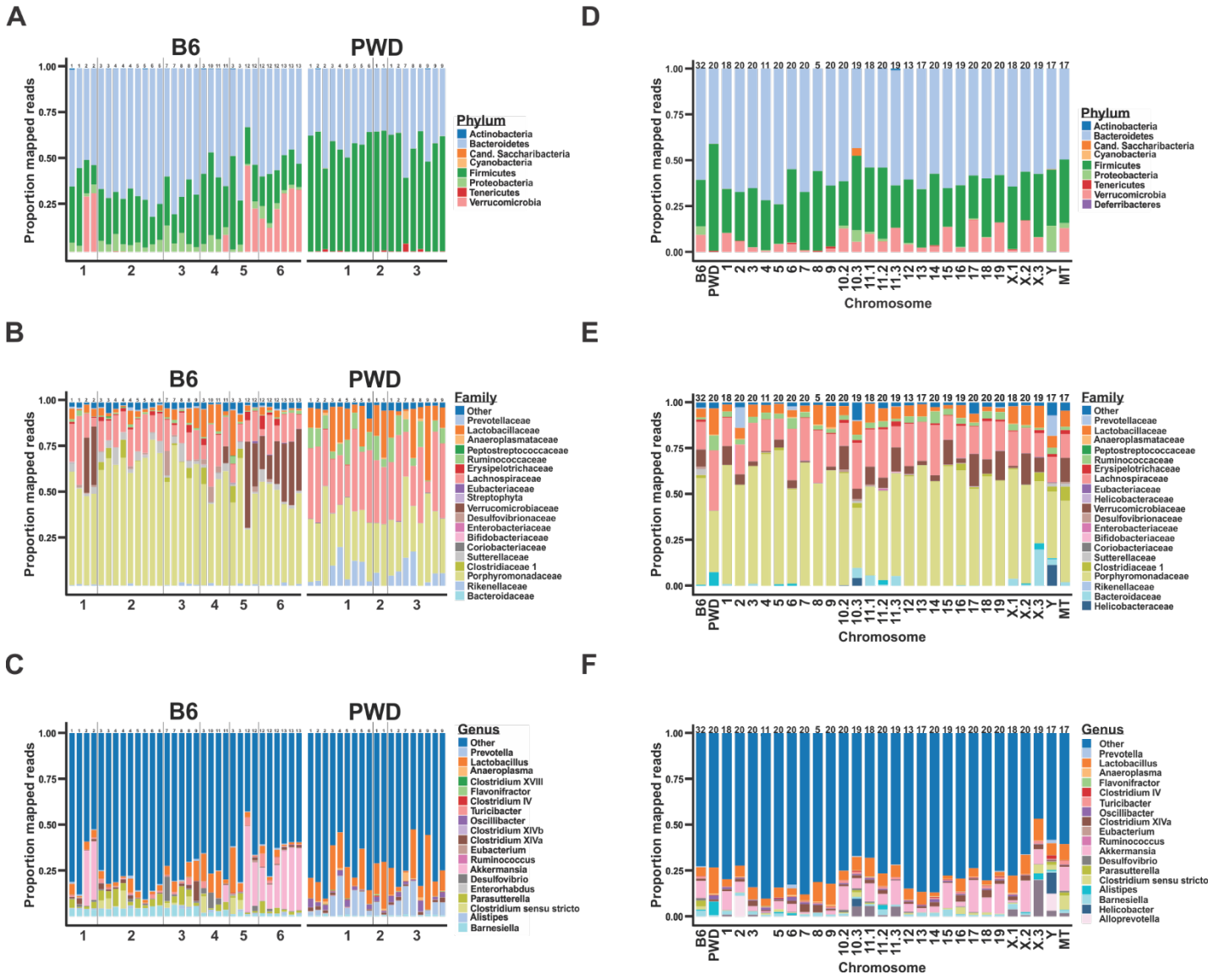

Figure S2

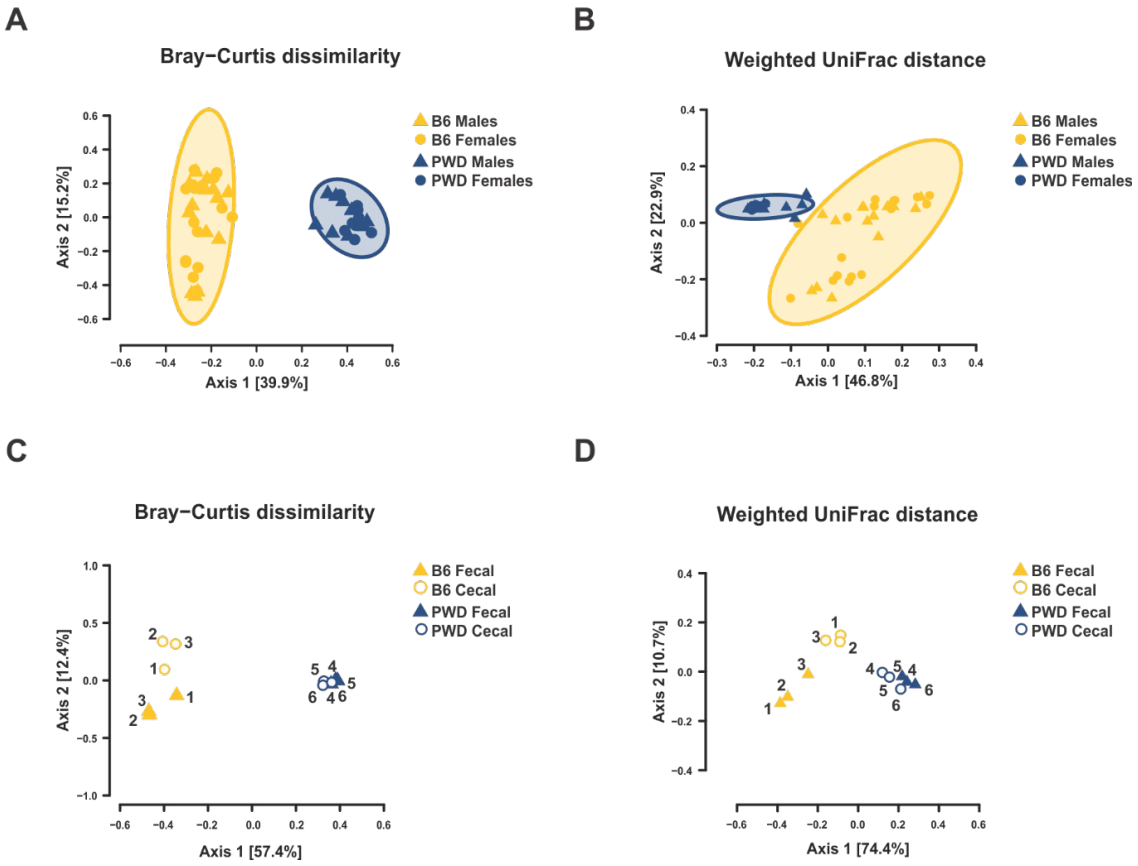

Figure S3

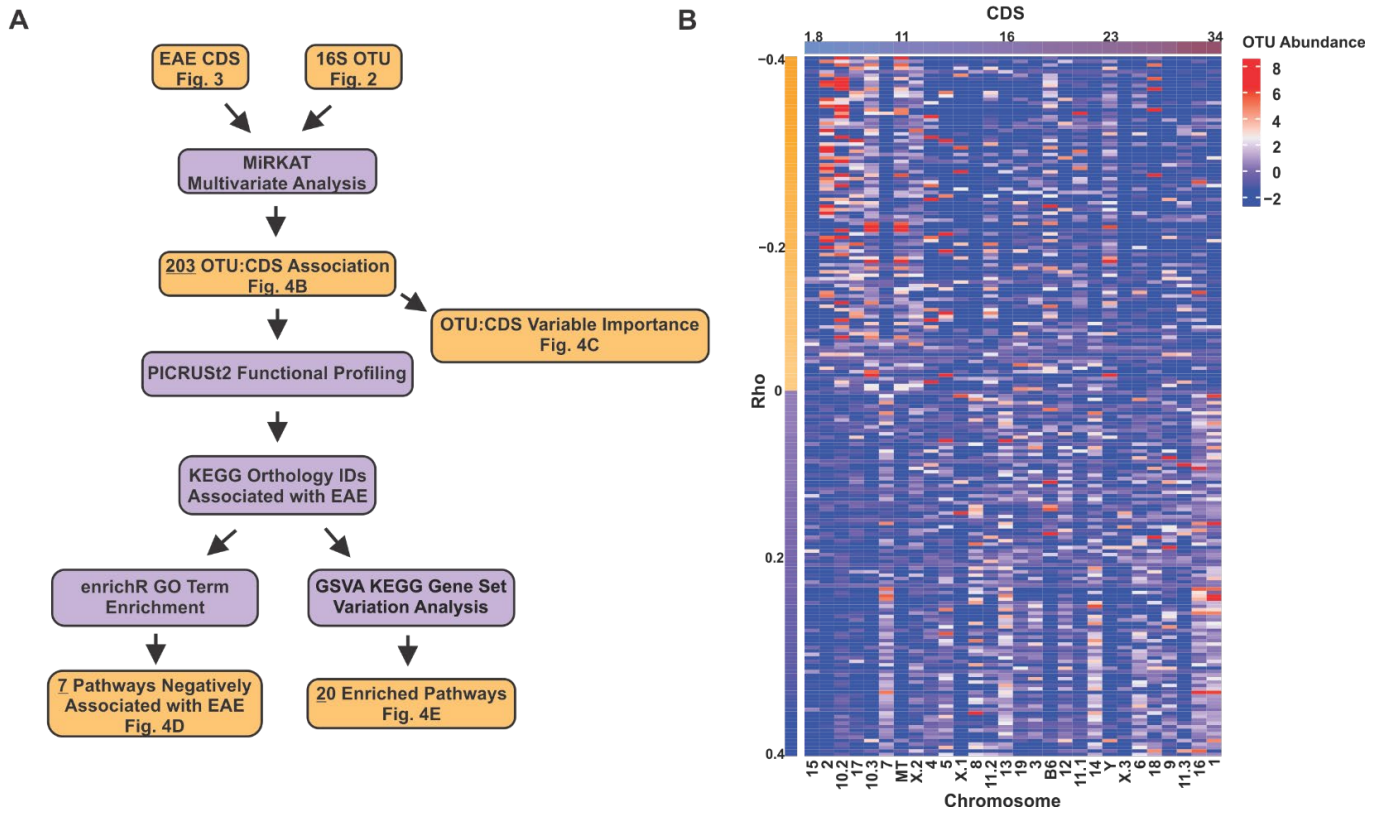

Figure S4

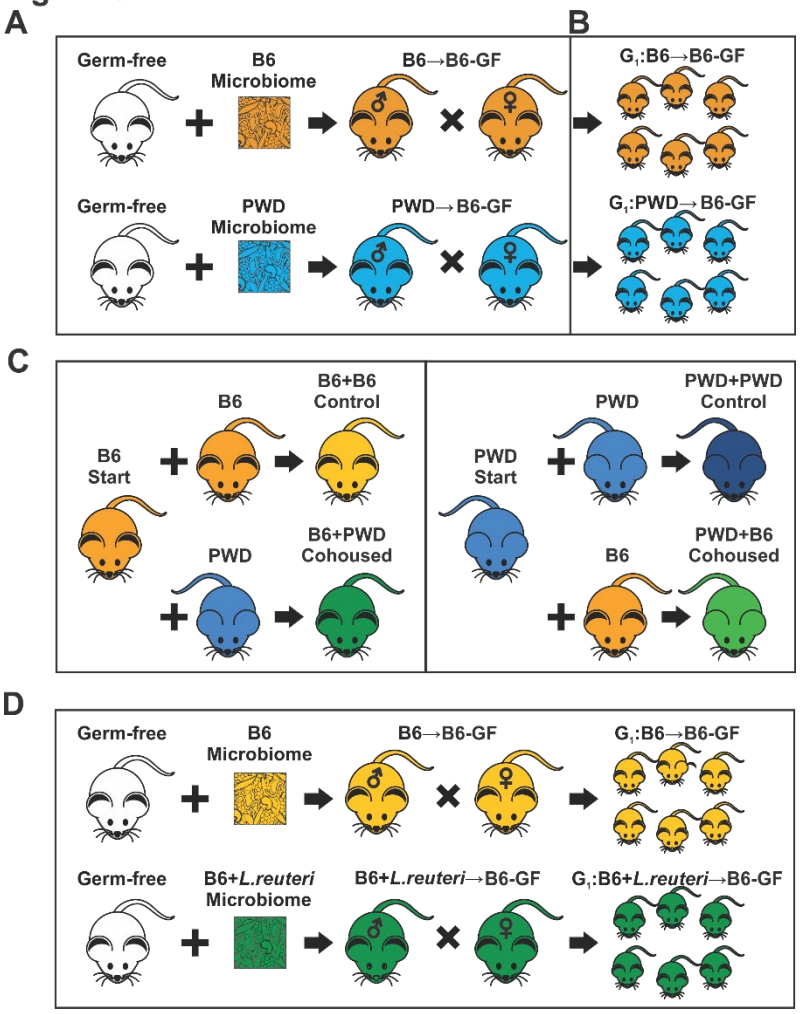

Figure S5

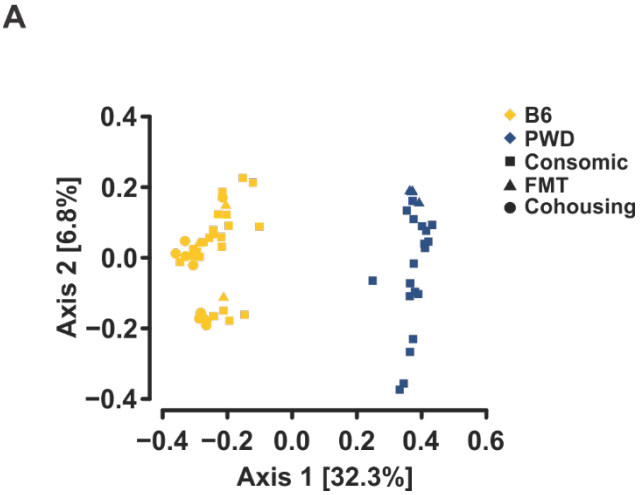

Figure S6

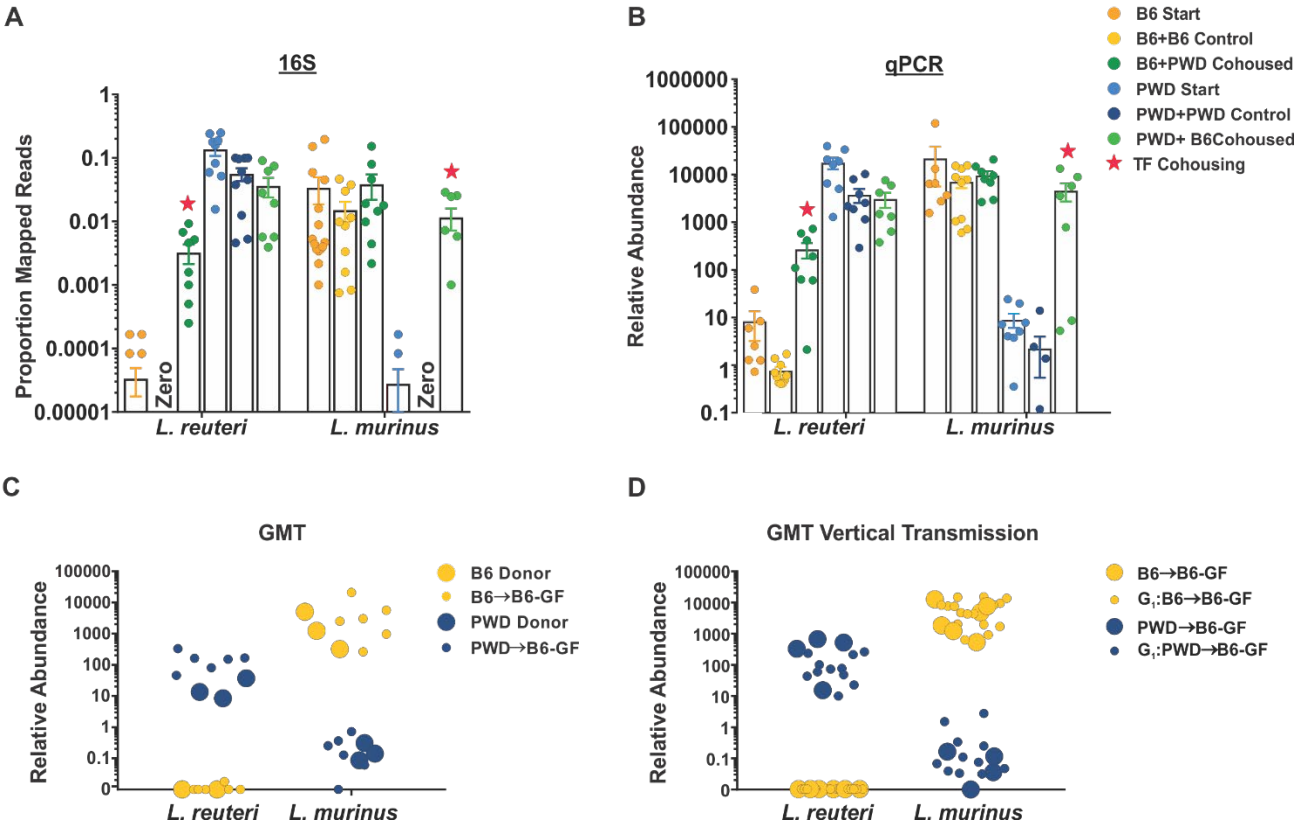

Figure S7

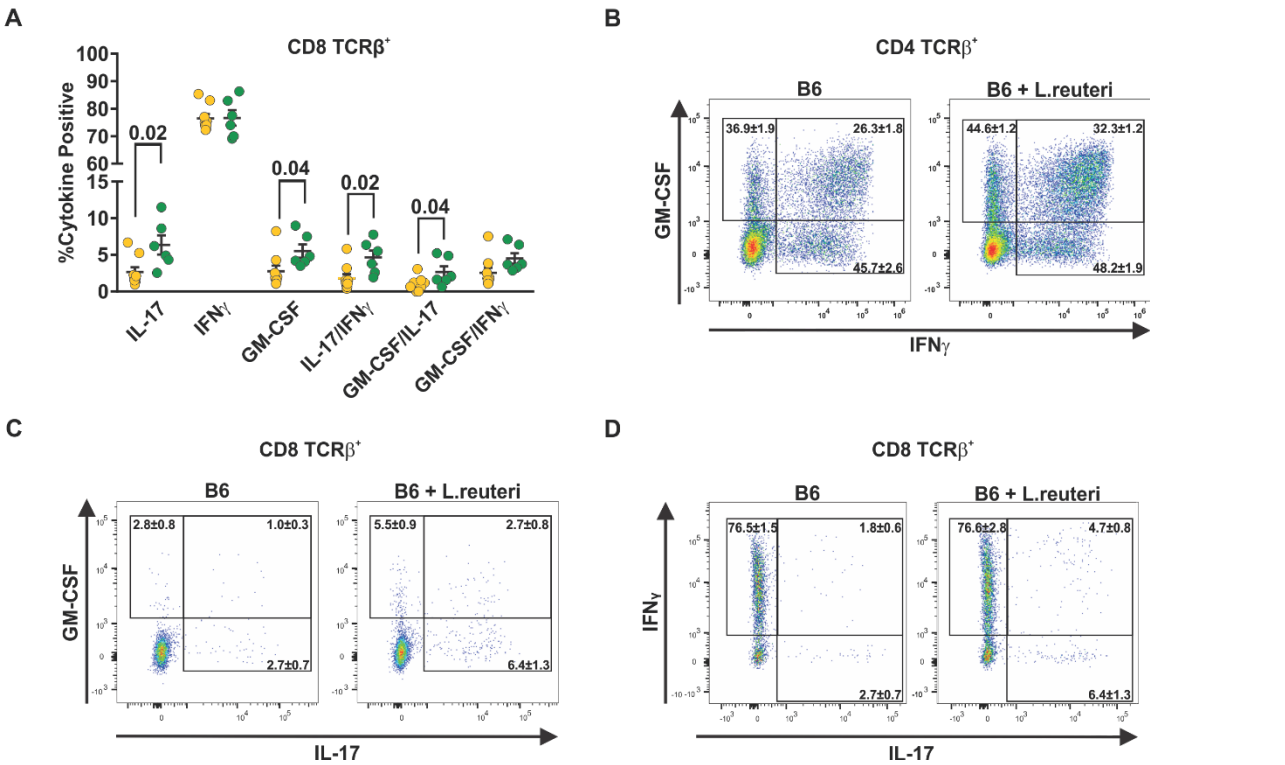

Figure S8

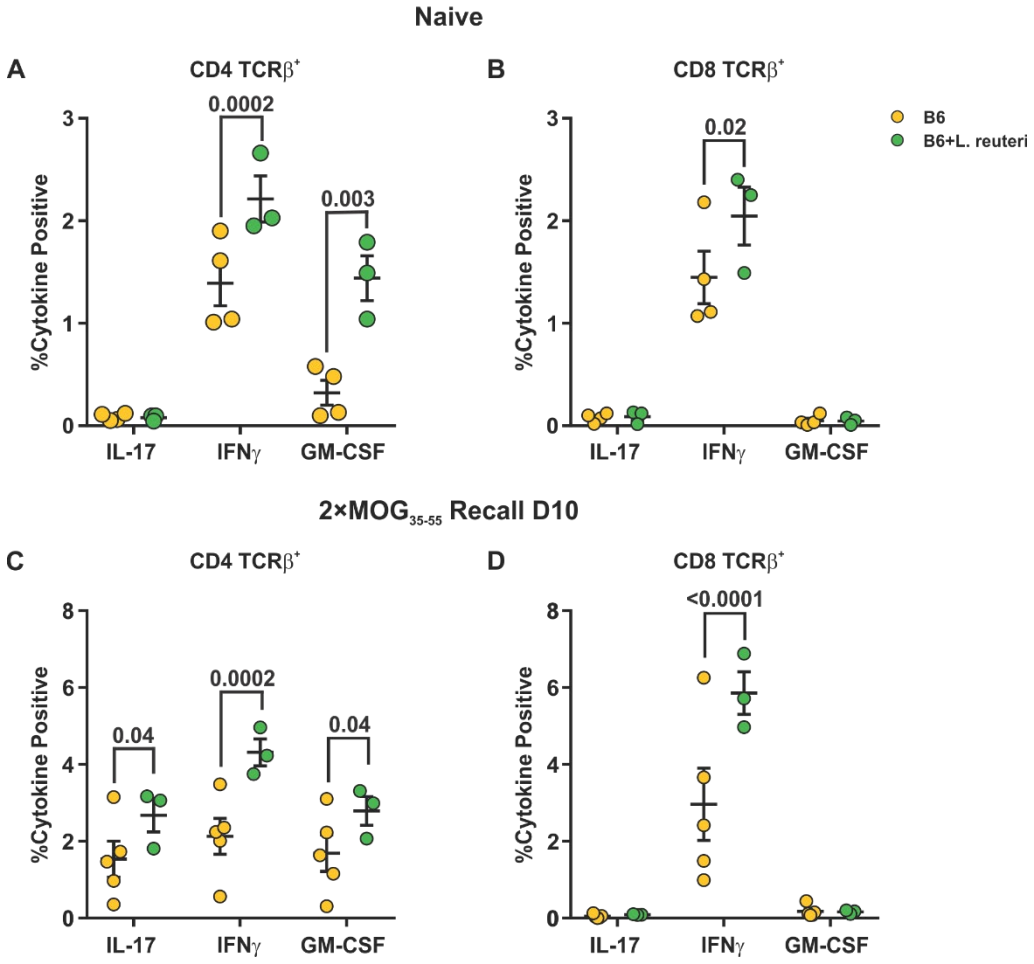

Figure S9

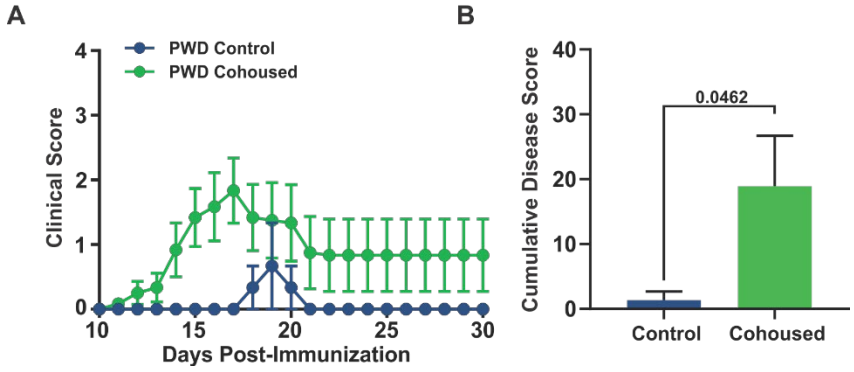

SUPPLEMENTAL REFERENCES

1. Krementsov DN, Asarian L, Fang Q, McGill MM, and Teuscher C. Sex-Specific Gene-by-Vitamin D Interactions Regulate Susceptibility to Central Nervous System Autoimmunity. *Front Immunol.* 2018;9:1622.
2. Krementsov DN, Case LK, Hickey WF, and Teuscher C. Exacerbation of autoimmune neuroinflammation by dietary sodium is genetically controlled and sex specific. *FASEB journal : official publication of the Federation of American Societies for Experimental Biology.* 2015.
3. Butterfield RJ, Sudweeks JD, Blankenhorn EP, Korngold R, Marini JC, Todd JA, et al. New genetic loci that control susceptibility and symptoms of experimental allergic encephalomyelitis in inbred mice. *J Immunol.* 1998;161(4):1860-7.
4. Butterfield RJ, Blankenhorn EP, Roper RJ, Zachary JF, Doerge RW, Sudweeks J, et al. Genetic analysis of disease subtypes and sexual dimorphisms in mouse experimental allergic encephalomyelitis (EAE): relapsing/remitting and monophasic remitting/nonrelapsing EAE are immunogenetically distinct. *J Immunol.* 1999;162(5):3096-102.
5. Rognes T, Flouri T, Nichols B, Quince C, and Mahe F. VSEARCH: a versatile open source tool for metagenomics. *PeerJ.* 2016;4:e2584.
6. Edgar RC, Haas BJ, Clemente JC, Quince C, and Knight R. UCHIME improves sensitivity and speed of chimera detection. *Bioinformatics (Oxford, England).* 2011;27(16):2194-200.
7. Edgar RC. UPARSE: highly accurate OTU sequences from microbial amplicon reads. *Nature methods.* 2013;10(10):996-8.
8. Edgar RC. Search and clustering orders of magnitude faster than BLAST. *Bioinformatics (Oxford, England).* 2010;26(19):2460-1.
9. Edgar RC. SINTAX: a simple non-Bayesian taxonomy classifier for 16S and ITS sequences. *bioRxiv.* 2016:074161.
10. Schloss PD, Westcott SL, Ryabin T, Hall JR, Hartmann M, Hollister EB, et al. Introducing mothur: open-source, platform-independent, community-supported software for describing and comparing microbial communities. *Applied and environmental microbiology.* 2009;75(23):7537-41.
11. Price MN, Dehal PS, and Arkin AP. FastTree 2 – Approximately Maximum-Likelihood Trees for Large Alignments. *PLOS ONE.* 2010;5(3):e9490.
12. Faith DP. Conservation evaluation and phylogenetic diversity. *Biological Conservation.* 1992;61(1):1-10.
13. McMurdie PJ, and Holmes S. phyloseq: An R Package for Reproducible Interactive Analysis and Graphics of Microbiome Census Data. *PLOS ONE.* 2013;8(4):e61217.
14. Love MI, Huber W, and Anders S. Moderated estimation of fold change and dispersion for RNA-seq data with DESeq2. *Genome biology.* 2014;15(12):550.
15. Dhariwal A, Chong J, Habib S, King IL, Agellon LB, and Xia J. MicrobiomeAnalyst: a web-based tool for comprehensive statistical, visual and meta-analysis of microbiome data. *Nucleic Acids Research.* 2017;45(W1):W180-W8.
16. Zhao N, Chen J, Carroll IM, Ringel-Kulka T, Epstein MP, Zhou H, et al. Testing in Microbiome-Profiling Studies with MiRKAT, the Microbiome Regression-Based Kernel Association Test. *American journal of human genetics.* 2015;96(5):797-807.
17. Douglas GM, Maffei VJ, Zaneveld J, Yurgel SN, Brown JR, Taylor CM, et al. PICRUSt2: An improved and extensible approach for metagenome inference. *bioRxiv.* 2019:672295.
18. Chen EY, Tan CM, Kou Y, Duan Q, Wang Z, Meirelles GV, et al. Enrichr: interactive and collaborative HTML5 gene list enrichment analysis tool. *BMC Bioinformatics.* 2013;14(1):128.
19. Hänzelmann S, Castelo R, and Guinney J. GSVA: gene set variation analysis for microarray and RNA-Seq data. *BMC Bioinformatics.* 2013;14(1):7.
20. Gu Z, Eils R, and Schlesner M. Complex heatmaps reveal patterns and correlations in multidimensional genomic data. *Bioinformatics (Oxford, England).* 2016;32(18):2847-9.
21. Cox LM, Yamanishi S, Sohn J, Alekseyenko AV, Leung JM, Cho I, et al. Altering the intestinal microbiota during a critical developmental window has lasting metabolic consequences. *Cell.* 2014;158(4):705-21.

22. Zelante T, Iannitti RG, Cunha C, De Luca A, Giovannini G, Pieraccini G, et al. Tryptophan catabolites from microbiota engage aryl hydrocarbon receptor and balance mucosal reactivity via interleukin-22. *Immunity.* 2013;39(2):372-85.
23. Wilck N, Matus MG, Kearney SM, Olesen SW, Forslund K, Bartolomaeus H, et al. Salt-responsive gut commensal modulates TH17 axis and disease. *Nature.* 2017;551:585.
24. Haarman M, and Knol J. Quantitative real-time PCR analysis of fecal Lactobacillus species in infants receiving a prebiotic infant formula. *Applied and environmental microbiology.* 2006;72(4):2359-65.
25. Gehrke S, Rice S, Stefanoni D, Wilkerson RB, Nemkov T, Reisz JA, et al. Red Blood Cell Metabolic Responses to Torpor and Arousal in the Hibernator Arctic Ground Squirrel. *J Proteome Res.* 2019;18(4):1827-41.
26. Nemkov T, Hansen KC, and D'Alessandro A. A three-minute method for high-throughput quantitative metabolomics and quantitative tracing experiments of central carbon and nitrogen pathways. *Rapid Commun Mass Spectrom.* 2017;31(8):663-73.
27. Nemkov T, D'Alessandro A, and Hansen KC. Three-minute method for amino acid analysis by UHPLC and high-resolution quadrupole orbitrap mass spectrometry. *Amino Acids.* 2015;47(11):2345-57.
28. Chong J, Soufan O, Li C, Caraus I, Li S, Bourque G, et al. MetaboAnalyst 4.0: towards more transparent and integrative metabolomics analysis. *Nucleic Acids Research.* 2018;46(W1):W486-W94.